

Chapter 4

Implementation and Experimental Set-up

4.1 Overview

All the relevant mathematical descriptions for digital recording and numerical reconstruction have been discussed in the last chapter. In this chapter, after a discussion on the recording requirements with the CCD camera, the capturing software, and the *Tag Image File Format* (TIFF), an experiment to implement what have been presented in the last chapter is shown. A simple off-axis holography experiment is carried out. In this experiment, the Fresnel holograms are recorded directly on to the CCD-sensor and stored electronically in the digital image processing system memory. Then, the reconstruction of these digitally sampled holograms is carried out numerically as described by Equation (3.25).

Follow by this is the implementation of digital holographic interferometry, where out-of-plane displacement of a cantilever beam is used as an example. Two different states of the cantilever beam is recorded directly on the CCD-sensor and numerically reconstructed to produce interference pattern. Two different approaches to calculate the intensity and interference phase of the two digitally sampled holograms are carried out.

4.2 Recording of the Off-axis Fresnel Hologram on a CCD-sensor

4.2.3 Recording requirements

The CCD camera system used throughout the experiment is the Sony CCD camera module XC-75 system, which is a monochrome video camera module using a CCD solid state image sensor. The relevant specifications of the CCD camera are given in Table 4-1.

Table 4-1 Specifications of the Sony CCD Monochrome Video Camera Module XC-75 Imaging System.

Effective picture elements	768×494 (horizontal/vertical)
Sensing area	1/2-inch size
Cell size	8.4×9.8μm (horizontal/vertical)
Chip size	7.95×6.45μm (horizontal/vertical)

The maximum spatial frequency in a hologram is determined by the wavelength and maximum angle θ_{\max} between the interfering waves. According to the sampling theorem the maximum spatial frequency f_{\max} that can be resolved by the CCD camera is limited by their pixel or cell size as given by Equation (3.12). The cell size of the CCD camera is 8.4μm horizontally and 9.8μm vertically; therefore

according to Equation (3.12) the maximum spatial frequencies for horizontal and vertical direction is

$$f_{\max}(\text{horizontal}) = \frac{1}{2 \times 8.4 \mu\text{m}} \cong 60 \text{mm}^{-1}$$

$$f_{\max}(\text{vertical}) = \frac{1}{2 \times 9.8 \mu\text{m}} \cong 51 \text{mm}^{-1}$$

As a numerical example use a wavelength $\lambda = 0.632 \mu\text{m}$. The maximum angle θ_{\max} between the reference and the object waves, according to Equation (3.11), is

$$\theta_{\max}(\text{horizontal}) = 2 \sin^{-1} \left(\frac{0.6328 \mu\text{m}}{2 \times 2 \times 8.4 \mu\text{m}} \right) \cong 2.2^\circ$$

$$\theta_{\max}(\text{vertical}) = 2 \sin^{-1} \left(\frac{0.6328 \mu\text{m}}{2 \times 2 \times 9.8 \mu\text{m}} \right) \cong 1.8^\circ$$

For the off-axis configuration of Figure 4-1, the object at a distance d of 1m away from the CCD-target must be smaller than 4cm. Larger objects have to be placed further apart from the CCD-target. So, in order to let the CCD resolved the entire object, which is placed at a distance a meter away from the CCD-target, the dimension of the objects must not be bigger that 4cm. For a distance d of about 50cm, the size of the object must not be bigger than 2cm.

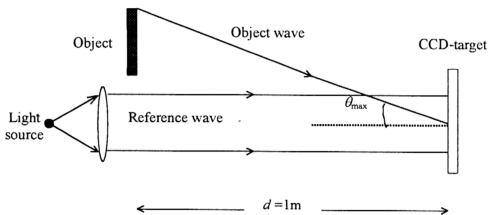


Figure 4-1 Off-axis configuration for digital holography.

4.2.2 Capturing software

The hologram is captured with the CCD camera, which is controlled by the F64PRO Edition 1.0 software. F64PRO is a Windows demonstration application that provides a large set of control functions for the Oculus F/64, which is a high performance image acquisition and processing board for the ISA 16-bit bus.

The Oculus F/64 is capable of acquiring data at a rate of up to 40 million pixels per second. For the present CCD camera, which has a capture resolution of 768×494 , the maximum capture speed is 25 frames/sec.

Figure 4-2 shows a software frame with the Acquisition Menu dropped down. By selecting Live Grab function, the continuous acquisition mode is started and the live image (hologram) is viewed from the display monitor. The Freeze function is used to capture and freeze the hologram. The hologram that has been captured is

digitized to an array of 512×512 pixels, each with 256 gray scale levels. Then the digitized hologram is stored in the digital image processing system memory as TIFF file image.

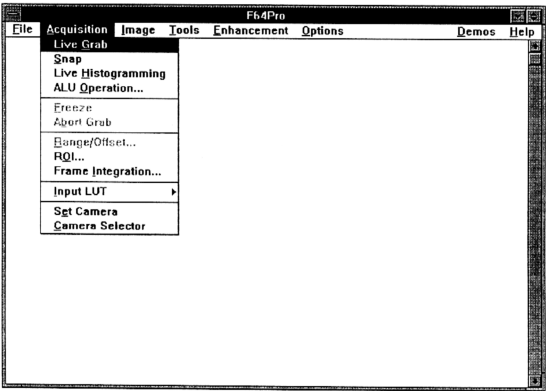


Figure 4-2 The frame outline of F64PRO software

4.2.3 Tag Image File Format (TIFF)

Tag Image File Format (TIFF) is one of the most common digital file formats used in digital image processing. In this image file format, a file is defined to be a sequence of 8-bit bytes, where the bytes are numbered from 0 to N. The largest possible TIFF file is 2^{32} bytes in length. A TIFF file begins with an 8-byte *Image File Header* that points to the *Image File Directories* (IFD.) An IFD contains information about the image, as well as pointers to the actual image data.

Basically, a TIFF image file is composed of several entries, each of which has tag and some associated data. Each entry's tag indicates the purpose of its associated data. The tag and their data are used to define an image's format and size, as well as many other parameters including the image data itself. The logical organization of a TIFF image file is shown in Figure 4-3.

Start of TIFF File

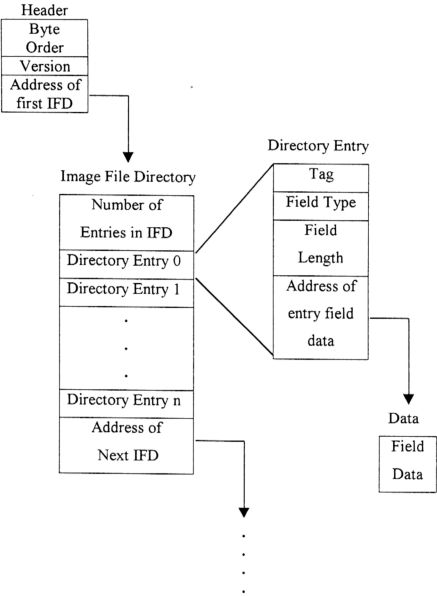


Figure 4-3 The organization of a TIFF image file.

4.2.3.1 Image File Header (IFH)

A TIFF file begins with an 8-byte *Image File Header* (IFH), containing the following information:

Bytes 0-1:	Indicates the byte order used within the file. Legal values are “II” and “MM”. In the “II” format, byte order is always from the least significant byte to the most significant byte. In the “MM” format, byte order is always from the most significant to the least significant, for both 16-bit and 32-bit integers.
Bytes 2-3:	Identifies the TIFF version number, i.e. 42.
Bytes 4-7:	Indicates the offset (in bytes) of the first IFD. The directory may be at any location in the file after the header.

The term byte offset is always used in this image file format to refer to a location with respect to the beginning of the TIFF file. The first byte of file has an offset of 0.

4.2.3.2 Image File Directory (IFD)

The *Image File Directory* (IFD) consists of a 2-bytes count of the number of directory entries (i.e., the number of fields), followed by a sequence of 12-byte field entries, followed by a 4-byte offset of the next IFD (or 0 if none).

There must be at least one IFD in a TIFF file and each IFD must have at least one entry (see Figure 4-3). Each IFD entry is a 12-byte record that contains a specific piece of information about the data. This 12-byte IFD entry has the following format:

Bytes 0-1:	The Tag that identifies the field.
Bytes 2-3:	The field Type.
Bytes 4-7:	The number of values, <i>Length</i> or <i>Count</i> of the indicted Type.
Bytes 8-11:	The Value Offset the file offset (in bytes) of the Value for the field. This file offset may point anywhere in the file.

There are numerous *Tags* that define the parameters, and the data, of the image stored in the TIFF file. Table 4-2 lists several commonly used *Tags* for storing a grey-scale image.

The field *Type* defines the type of data. The following are the field *Types* and their sizes:

1 = BYTE	8-bit unsigned integer.
2 = ASCII	8 bit byte that contains a 7-bit ASCII character.
3 = SHORT	16-bit (2-byte) unsigned integer.
4 = LONG	32-bit (4-byte) unsigned integer.
5= RATIONAL	Two LONGs: the first represents the numerator of fraction; the second, the denominator

The field *Length* or *Count* is the number of data items contained in the field data.

The *Offset* or *Address* of field data is the location, relative to the beginning of the file, of the data associated with the tag. The digitized hologram is stored in the field data named *StripOffsets*, which tag number is 273. During the reconstruction process, the information of the digital hologram that has been stored is extracted from this field data.

Table 4-2 Common TIFF Gray Scale Image Tags

Tag Name	Tag Number
<i>ImageWidth</i>	256
<i>ImageLength</i>	257
<i>BitsPerSample</i>	258
<i>Compression</i>	259
<i>PhotometricInterpretation</i>	262
<i>ImageDescription</i>	270
<i>StripOffsets</i>	273
<i>RowsPerStrip</i>	278
<i>StripByteCounts</i>	279
<i>Xresolution</i>	282
<i>Yresolution</i>	283
<i>ResolutionUnits</i>	296

4.2.4 Recording procedures

Figure 4-4 shows a simple arrangement for recording the off-axis holograms. The experimental investigation is carried out with a 20-mW HeNe laser. The light from the laser is divided by mean of a beam splitter into a reference wave and an object-illuminating beam. The reference beam is expanded with a telescope and collimated with a lens to become a plane wave, and illuminates on to the CCD-sensor.

The objects used in the experiments are a black tag with the letters UM in white on it (as shown in Figure 4-4) and a white and diffuse pyramid-shaped object, which were placed at a distance of about 1m from the CCD-target. The dimension of the objects used is about $2.5\text{cm} \times 1.5\text{cm}$ for the black sign and $2.0\text{cm} \times 1.0\text{cm} \times 1.0\text{cm}$ for the pyramid-shaped object.

The important initial step is to determine the intensity ratio between the reference beam and the object beam that illuminate on to the CCD-sensor. This is done by using the photosensitive diode to measure the intensity and also with the help of the real-time histogram and the display monitor. The display monitor allows one to view the interference pattern formed by the reference and the object beams.

After getting the optimum intensity ratio, the hologram is captured with the help of F64PRO software mentioned earlier. For Fast Fourier transform (FFT) algorithm, it is advantageous if the number of pixels in each row and in each column is a power of 2. Therefore with the help of the F64PRO software the hologram is digitised to an array of 512×512 pixel, each with 256 gray scale levels. The digitised hologram is stored as TIFF file image in the computer memory storage. Since the maximum capture speed of the CCD camera is 25 frames/sec, the experiments can be carried out without any vibration isolation.

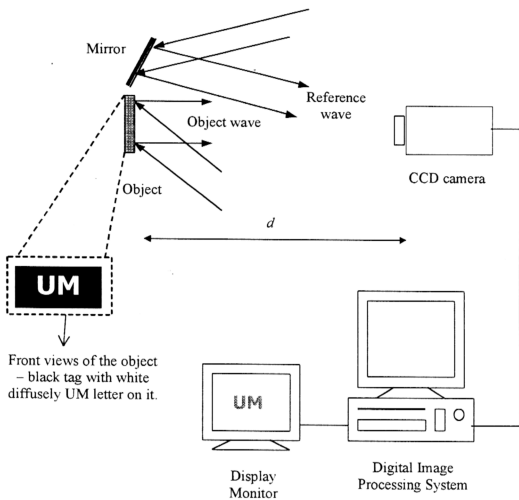


Figure 4-4 Experimental set-up for digital recording of an off-axis hologram.

4.3 Numerical Reconstruction of Digital Fresnel Hologram

The reconstruction of the digitally sampled Fresnel hologram, which is stored in the computer memory as TIFF file image, is carried out by the numerical evaluation of the two-dimensional discrete inverse Fourier transform equation as described by Equation (3.25) (reproduced below):

$$\Gamma(m, n) = \sum_{k=0}^{N-1} \sum_{l=0}^{N-1} \mathbf{t}(k, l) \exp \left[\frac{i\pi}{\lambda d} (k^2 \Delta x^2 + l^2 \Delta y^2) \right] \exp \left[-i2\pi \left(\frac{mk}{N} + \frac{nl}{N} \right) \right]$$

As mentioned in the last chapter, Equation (3.25) can be calculated with the standard fast Fourier transform (FFT) algorithm. The numerical reconstruction algorithm is written in C programming language [30]. Basically, the program consists of three major parts, as shown in Figure 4-5. The first step is to read out the amplitude transmittance $\mathbf{t}(k, l)$ from the digitally sampled hologram, which is stored as a TIFF file image. The information needed is stored in the location addressed by *StripOffsets*. The amplitude transmittance $\mathbf{t}(k, l)$ is read out and stored in a temporary file.

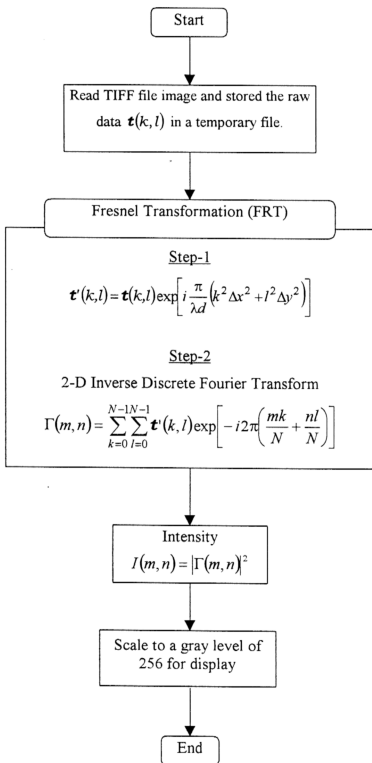


Figure 4-5 Flowchart of the numerical reconstruction of digital hologram.

The second part is the Fresnel transformation (FRT) routine, which calculates the complex amplitude $\Gamma(m, n)$ of the hologram according to the diffraction Equation (3.25) with an FFT algorithm. This routine consist two steps:

Step-1: The product of input data $\mathbf{t}(k, l)$ with the first exponential factor in the sum

of Equation (3.25) i.e. $\mathbf{t}(k, l) \exp \left[\frac{i\pi}{\lambda d} (k^2 \Delta x^2 + l^2 \Delta y^2) \right]$ is calculated.

Step-2: Using the Fast Fourier Transform (FFT) algorithm, the 2-D inverse discrete Fourier transform of the product from Step-1 is calculated.

Finally, the intensity distribution $I(m, n)$ is calculated according to Equation (3.26), and scaled to a gray level of 256 for display.

4.4 Results and Discussions

4.4.1 Read TIFF file image's program

Table 4-3 shows a print out of a partial TIFF image file (digitally sampled hologram) information. VAX order indicated that the Byte Order is II; Version 42 indicated that the image file is TIFF; and Image File Directory indicated that the first File Directory is at 8 bytes from the beginning of the file.

The dimension of the digitally sampled hologram is 512×512 bytes. The data is stored in 32 strips with each strip has 16 rows and 8192 bytes. The first strip is started at the location 1966 bytes from the beginning of the file, and the following strips are at the location given by:

$$n - \text{strip} = 1966 + (n-1)8192 \quad \text{where } n = 1, 2, \dots, 32$$

The last strip starts at the location 255918 bytes and ends at 264110 bytes from the beginning of the file. Thus, the needed hologram data, i.e. the amplitude transmittance $t(k, l)$, is stored in the location between 1966 bytes and 264100 bytes from the beginning of the file. These raw data is read out and stored in a temporary file for further processing.

Table 4.3 Partial TIFF file image information

VAX order.				
Version is 42.				
Image file directory at 8.				
Entry: TAG 256	TYPE 4	LENGTH 1	SIZE 4	
Image width = 512				
Entry: TAG 257	TYPE 4	LENGTH 1	SIZE 4	
Image length = 512				
Entry: TAG 258	TYPE 3	LENGTH 1	SIZE 2	
Bits Per Sample = 8				
Entry: TAG 259	TYPE 3	LENGTH 1	SIZE 2	
Compression = 1				
Entry: TAG 262	TYPE 3	LENGTH 1	SIZE 2	
Photometric Interpretation = 3				
Entry: TAG 273	TYPE 4	LENGTH 32	SIZE 128	
Offset value is 158				
Strip Offsets = 158				
Strip 0 Offset 1966				
Entry: TAG 278	TYPE 4	LENGTH 1	SIZE 4	
Row per Strip = 16				
Entry: TAG 279	TYPE 4	LENGTH 32	SIZE 128	
Offset value is 286				
Strip Byte Counts = 286				
Strip 0 Count 8192.				
Number of strips = 32 length 32				
Entry: TAG 282	TYPE 4	LENGTH 1	SIZE 8	
Offset value is 414				
X resolution = 100/100				
Entry: TAG 283	TYPE 5	LENGTH 1	SIZE 8	
Offset value is 422				
Y resolution = 100/100				
Entry: TAG 296	TYPE 3	LENGTH 1	SIZE 2	
Resolution unit = 1				

4.4.2 Numerical reconstruction results and discussions

Figure 4-6(a) and Figure 4-7(a) shows a part of a digitally sampled hologram for white UM-letter tag and pyramid-shaped object. These pictures are printed out from the monitor of the digital image processing system. The original dimensions of the whole holograms were $7.95\text{mm} \times 6.45\text{mm}$, which are the dimensions of the CCD-chip.

The numerical reconstruction for each digital hologram according to Equations (3.25) and (3.26) is demonstrated in Figure 4-6(b) and Figure 4-7(b). A real image of the white UM-letter tag and pyramid-shaped object together with the reference beam is noticeable. Because of the off-axis geometry, these two parts of the real image are separated (Figure 4-7(b)). The quality of the reconstructed image show in the Figure 4-6 and Figure 4-7 were limited by the quality of the printing. The images can be seen more clearly on the display monitor although their qualities are not the good.

These experiments demonstrate that the CCD cameras are in principle suitable as a recording medium for holograms. Due to the low spatial resolution, the applicability of the CCD camera is still limited to the small objects at a large distance from the target.

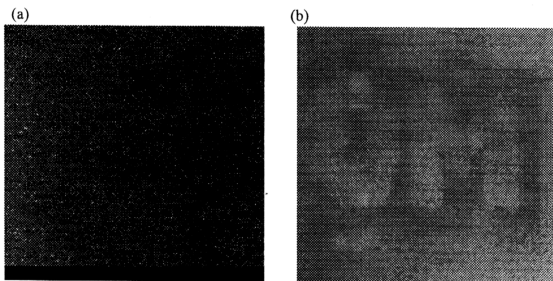


Figure 4-6 (a) Digital sampled hologram and (b) numerical reconstruction – intensity of white UM-letter tag.

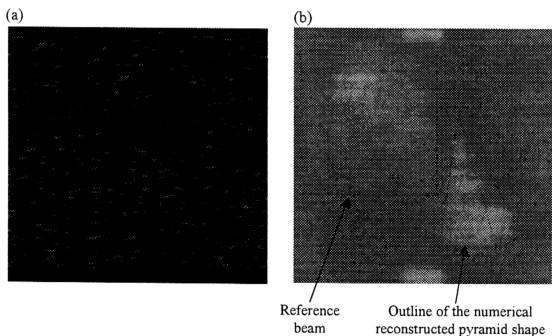


Figure 4-7 (a) Digital sampled hologram and (b) numerical reconstruction – intensity of pyramid-shaped object.

4.5 Digital Holographic Interferometry

4.5.1 Digital recording

The experimental set-up for implementation of digital holographic interferometry is shown in Figure 4-8. The set-up is similar to that used in the previous section for recording a single hologram. But now the object in this experiment is a cantilever beam, which is clamped at the base and loaded at the free end. The dimension of the cantilever beam was $2.5\text{cm} \times 1.5\text{cm}$. The cantilever was placed at a distance of about a meter from the CCD-target. The load is applied with a micrometer screw into the direction of the CCD. The direction of illumination and observation are nearly perpendicular to the object surface and parallel to each other. The experiment set-up is sensitive to the out-of-plane displacement.

The procedures for digital hologram recording is similar to that described in the previous chapter. In holographic interferometry, instead of a single hologram, two holograms are recorded. First, the undistorted state of the cantilever is recorded. Before the second hologram is recorded, the cantilever is bent a few microns to produce the distorted state of the cantilever. Both of these holograms are stored separately in a digital image processing system memory.

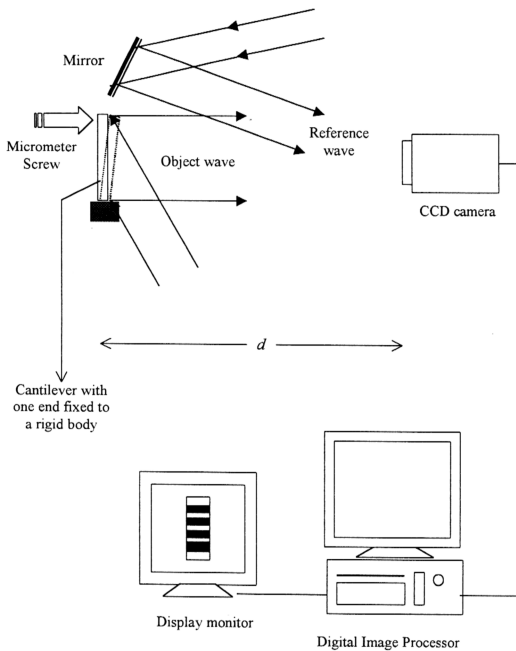


Figure 4-8 Experimental set-up for digital recording of an off-axis hologram of a cantilever.

4.5.2 Numerical reconstruction

As mentioned in Section (3.4), there are two ways to process the digitally stored holograms in digital holographic interferometry. First, the two holograms are superimposed as described by Equation (3.28) before the numerical reconstruction to form an interferogram. Secondly, each object state is reconstructed separately and the phase is calculated with Equation (3.27). The interference phase is then calculated with Equation (3.29).

Figure 4-9 shows the numerical reconstruction flowchart of the first approach to produce interferogram. Basically, it consisted of four major steps. First, the amplitude transmittances $t_1(k, l)$ and $t_2(k, l)$ are read from the two digitally stored holograms and the raw data is stored separately, as described in previous chapter. The second step is the superposition of these amplitude transmittances to form the resultant amplitude transmittance $t(k, l)$. The third step is the Fresnel Transformation (FRT) routine, which calculates the complex amplitude $\Gamma(m, n)$ of the hologram. The final step is to calculate the intensity distribution $I(m, n)$ and scales the result to a gray level of 256 for display.

Figure 4-10 shows the numerical reconstruction flowchart of interference phase. It also consisted of four major steps. First, the amplitude transmittances $t_1(k, l)$ and $t_2(k, l)$ are read from the two digitally stored holograms. The second step is the Fresnel Transformation (FRT) routine, which calculates the complex amplitude $\Gamma(m, n)$ of the hologram. The next step is to calculate the phase $\Phi(m, n)$ of each hologram. In the final step, the interference phase $\Delta\Phi(m, n)$ is calculated by subtracting the reconstructed phases of the undistorted and distorted state and scales the result to a gray level of 256 for display.

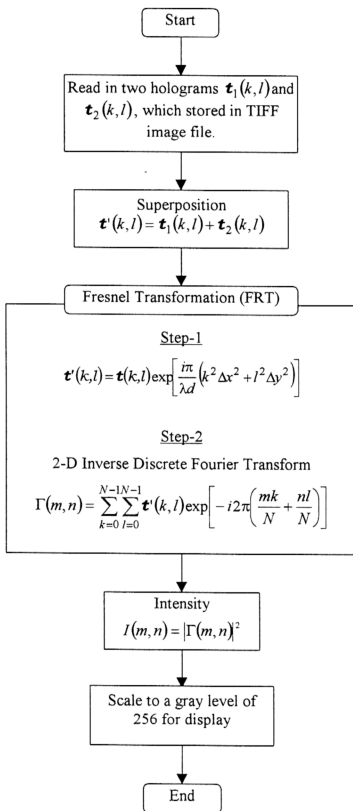


Figure 4-9 Flowchart of the numerical reconstruction of the first approach to produce holographic interferogram.

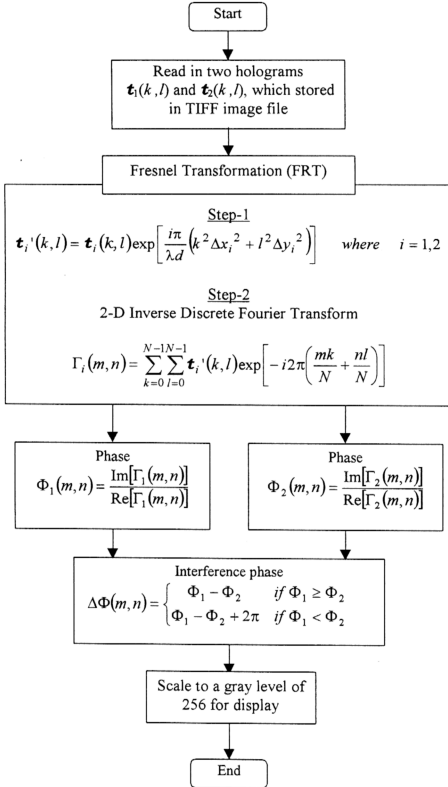


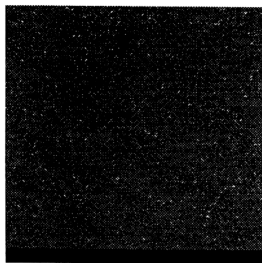
Figure 4-10 Flowchart of numerical reconstruction of the second approach to produce an interference phase.

4.5.3 Results and discussions

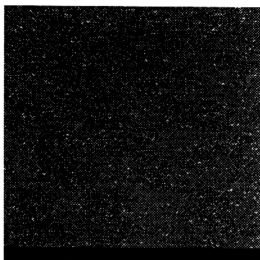
Figure 4-11 and Figure 4-12 shows the results of the reconstruction process. Figures 4-11(a) and (b) show the digitally sampled holograms at two different loading states. Figure 4-11(c) shows a part of the digital hologram resulting from the superposition of the two digital holograms. The original dimensions of the whole hologram are 7.95mm×6.45mm, which are the dimensions of the CCD-chip. The numerical reconstruction of the sum of these holograms with Equations (3.25), (3.26) and (3.28) results in an interference fringe pattern, as shown in Figure 4-11(d). This interference fringe pattern is the numerical counterpart to an optically reconstructed double-exposed hologram.

For quantitative measurements of deformations, the interference phase is of interest and not the intensity. For determining the interference phase, the phases of each individual object state are calculated with Equations (3.25) and (3.27). These numerically reconstructed results are shown in Figures 4-12(a) and (b). A white point in these figures corresponds to a phase value of 2π . A black point represents a phase value of 0. Subtraction of these phases with Equation (3.29) results in the interference phase that shown in Figure 4-12(c). To improve the results, the phase is smoothened with a median filter. The quality of the reconstructed and filtered phase in Figure 4-12(d) is comparable with that of conventional techniques of hologram interferometry – phase-shifting methods.

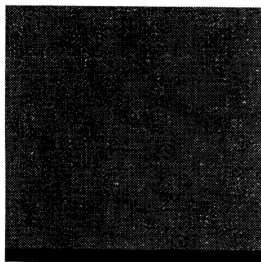
The interference phase is indefinite to an additive multiple of 2π . Figure 4-13 shows a one-dimensional interference phase modulo 2π . Noise is smoothen with the median filter (Figure 4-13(b)). In these figures, the vertical axis of the *Line Morphometry* is the intensity in 256 gray scale and the horizontal axis is the position of the cantilever beam.



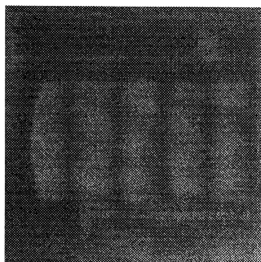
(a) $t_1(k, l)$



(b) $t_2(k, l)$

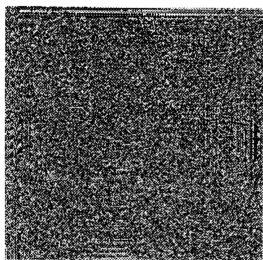


(c) $t(k, l) = t_1(k, l) + t_2(k, l)$

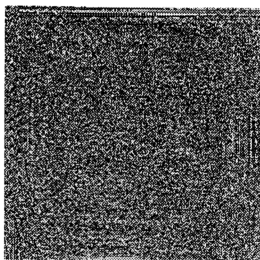


(d) $I(k, l)$

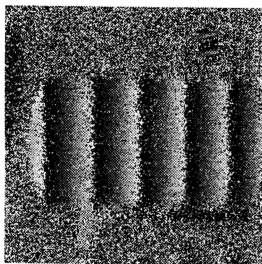
Figure 4-11 Digitally sampled hologram (a) before, (b) after deformation, and (c) superposition of (a) and (b). Figure (d) is the result of numerical reconstruction of digital hologram (c) that clearly shows the interference pattern.



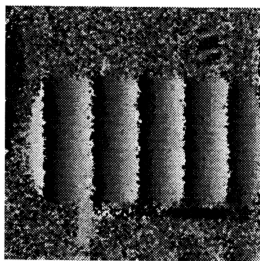
(a) $\Phi_1(m,n)$



(b) $\Phi_2(m,n)$



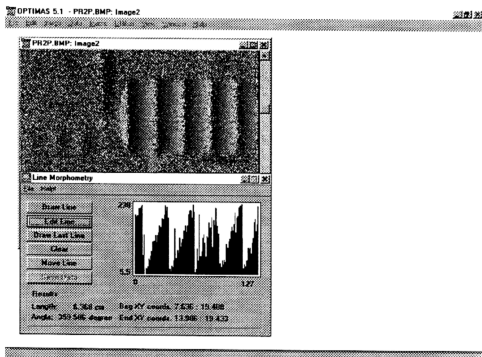
(c) Interference phase $\Delta\Phi(m,n)$



(d) After median filtering

Figure 4-12 Numerical reconstruction of phase: (a) before deformation, and (b) after deformation. Figure (c) shows the interference phase, and (d) shows interference phase after median filtering.

(a)



(b)

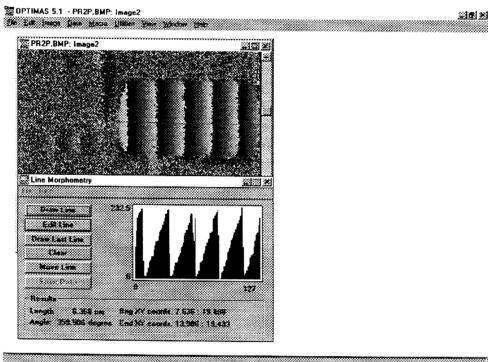


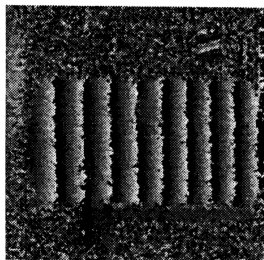
Figure 4-13 Interference phase modulo 2π (a) calculated directly from the holograms; (b) median filtered and their Line Morphometry.

Figure 4-14 shows the different loaded interference phases. It is clearly shown that the increase of the out-of-plane displacement of the cantilever gives more interference fringe pattern. In Figure 4-14(d) the number of fringe was so crowded and became difficult to count.

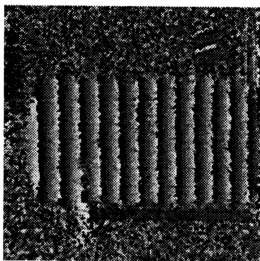
The digital recording and numerical reconstruction have some advantages compared with photographic recording and optical reconstruction. No chemical or physical processes for developing are necessary, and the reconstruction can be made without a light source. Moreover, the reconstructed image is available in a digital form, which is useful for digital holographic interferometry.

Digital recording and numerical reconstruction of holograms offer new possibilities to optical metrology. From two Fresnel holograms, which are recorded digitally in two different states of the object, the interference phase can be calculated directly. This is possible because not only the intensity but also the phase of each individual state is reconstructed. The interference phase results from a comparison of these individual phases. A holographic interferogram is created if the holograms are superimposed numerically and are reconstructed jointly. This means that one can choose the evaluation techniques in the reconstruction process. Therefore, it is expected that other fringe patterns of laser metrology, such as shearography, speckle photography fringes, can also be generated from the digital holograms.

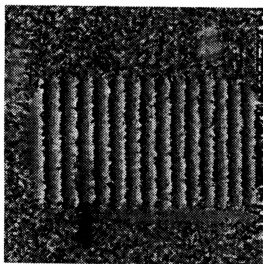
The main advantage of digital holography is that the phase can be calculated from one single recording, so that a phase-shifting unit, for generating phase-shifted interferograms, is not required. The digital recording and numerical reconstruction can be integrated into one system.



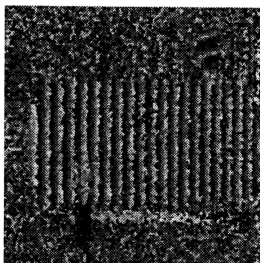
(a)



(b)



(c)



(d)

Figure 4-14 Interference phase from the cantilever with different loads.
The loading increases from (a) to (d).

The major drawback of the method is the low spatial resolution of CCD arrays. Therefore, the angle between the reference and object waves must be limited to a few degrees. Consequent, only small objects and at large distance from the CCD-target can be resolved. However, with the present CCD camera, the quality of the reconstructed image is comparable to that of conventional holographic techniques using photographic plates.